OXYGEN ISOTOPE MEASUREMENTS OF A RARE MURCHISON TYPE A CAI AND ITS RIM. J. E. P. Matzel[1], J. I. Simon[2], I. D. Hutcheon[1], B. Jacobsen[1], S. B. Simon[3], and L.Grossman[3]. [1]Lawrence Livermore National Lab, 7000 East Ave, Livermore, CA 94550, USA, matzel2@llnl.gov, [2]NASA Johnson Space Center, Houston, TX 77058, USA, [3]The University of Chicago, Chicago, IL 60637, USA.

Introduction: Ca-, Al-rich inclusions (CAIs) from CV chondrites commonly show oxygen isotope heterogeneity among different mineral phases within individual inclusions reflecting the complex history of CAIs in both the solar nebula and/or parent bodies [1]. The degree of isotopic exchange is typically mineral-specific, yielding ^{16}O-rich spinel, hibonite and pyroxene and ^{16}O-depleted melilite and anorthite. Recent work [1] demonstrated large and systematic variations in oxygen isotope composition within the margin and Wark-Lovering rim of an Allende Type A CAI. These variations suggest that some CV CAIs formed from several oxygen reservoirs and may reflect transport between distinct regions of the solar nebula or varying gas composition near the proto-Sun.

Oxygen isotope compositions of CAIs from other, less-altered chondrites show less intra-CAI variability and ^{16}O-rich compositions [2-3]. The record of intra-CAI oxygen isotope variability in CM chondrites, which commonly show evidence for low-temperature aqueous alteration, is less clear, in part because the most common CAIs found in CM chondrites are mineralogically simple (hibonite ± spinel or spinel ± pyroxene) and are composed of minerals less susceptible to O-isotopic exchange. No measurements of the oxygen isotope compositions of rims on CAIs in CM chondrites have been reported.

Here, we present oxygen isotope data from a rare, Type A CAI from the Murchison meteorite, MUM-1. The data were collected from melilite, hibonite, perovskite and spinel in a traverse into the interior of the CAI and from pyroxene, melilite, anorthite, and spinel in the Wark-Lovering rim. Our objectives were to (1) document any evidence for intra-CAI oxygen isotope variability; (2) determine the isotopic composition of the rim minerals and compare their composition(s) to the CAI interior; and (3) compare the MUM-1 data to oxygen isotope zoning profiles measured from CAIs in other chondrites.

MUM-1 Petrography: The petrography of MUM-1 (MUrchison Melilite) was previously described by MacPherson et al. [4], who reported that it is one of three small angular fragments so similar in texture and composition, they may be pieces of a single broken inclusion. MUM-1 is similar in mineralogy and composition to Allende compact Type A CAIs. The interior of MUM-1, away from the layered rim, consists primarily of blocky melilite crystals (~150 µm in length) that enclose euhedral spinel crystals (~20 µm), euhedral hibonite blades (~30-40 µm in length) and irregularly-shaped perovskite grains (~1-10 µm) (Fig. 1). Spinel tends to be slightly rounded and, in places, forms long chains. Hibonite and perovskite are sparse in the interior and are closely associated with spinel.

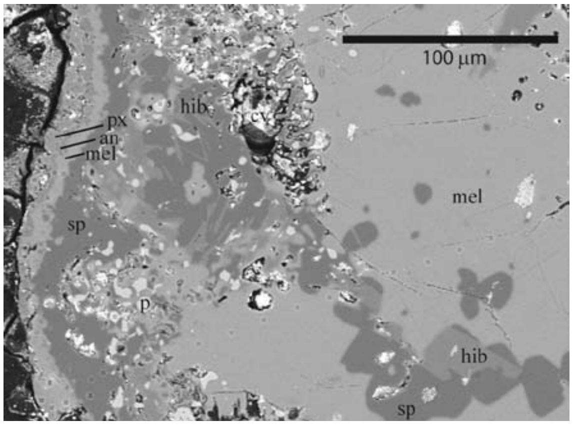

Figure 1. Backscattered electron image of MUM-1. Abbreviations are as follows: mel, melilite; an, anorthite; px, pyroxene; sp, spinel, p, perovskite; hib, hibonite, and cv, cavity.

Separating the melilite-rich, coarse-grained interior from the layered rim is a 30-70 µm thick margin rich in spinel, perovskite, hibonite and small (10-15 µm) rounded islands of melilite. Abundant perovskite grains are enclosed within dense regions of spinel and numerous needles and blades (~8-20 µm) of hibonite. A 25-30 µm-thick, layered rim sequence mantles the inclusion. This rim consists of the following (from inside to outside): spinel, melilite, anorthite and clinopyroxene grading outward in composition from Ti-, Al-rich to Ti-, Al-poor.

The predominant alteration feature is the presence of abundant vermicular cavities in the margin of the CAI. Because many of the melilite islands within the margin contain cavities, [4] suggested the latter were formed by selective removal of melilite. Cross-cutting veins containing secondary phases, common in coarse-grained Allende CAIs, are absent from MUM-1.

The MUM fragments are unique among Murchison refractory inclusions and resemble some Allende compact Type A inclusions in many respects [5]. They differ from the latter, however, in their higher hibonite and perovskite contents, the abundance of gehlenitic melilite, different secondary minerals and different rim sequence [4]. At the time the MUM fragments were discovered, the Mg isotope systematics of melilite and spinel were measured [6; Hutcheon, unpub data]. Data for spinel and melilite fall tightly along a correlation line with slope corresponding to $(^{26}Al/^{27}Al)_0 = (4.88 \pm 0.48) \times 10^{-5}$ (Fig. 2) and provide no indication that MUM-1 experienced sub-solidus Mg isotopic disturbance.

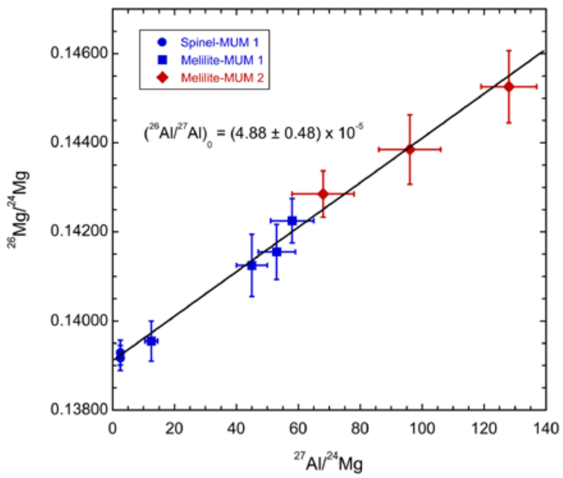

Figure 2. ^{26}Al-^{26}Mg evolution diagram for two fragments of the MUM CAI showing a regression line fitted to data from spinel and melilite. Uncertainties are 2σ.

Analytical Methods: Oxygen isotope abundances were determined using the Lawrence Livermore National Laboratory *Cameca* NanoSIMS 50. An ~15 pA primary Cs^+ beam was rastered over 2×2 μm^2 areas. Negative secondary ions were acquired by simultaneously measuring $^{16}O^-$ on a Faraday cup and $^{17}O^-$, $^{18}O^-$, and $^{28}Si^-$ on electron multipliers. The secondary ion intensities were corrected for background and counting system dead time. A mass resolving power of ~6600 was used to minimize the contribution from $^{16}OH^-$ to $^{17}O^-$. Instrumental mass fractionation was determined by measuring terrestrial standards including Burma spinel, Miakejima anorthite, and San Carlos olivine. The external precision of our standards was <4.4 ‰ (2SD) for both $\delta^{17}O$ and $\delta^{18}O$; precision on $\Delta^{17}O$ was <4.0 ‰ (2SD) for all three standards, and the difference in $\Delta^{17}O$ among the terrestrial minerals was <0.5 ‰, much less than our typical uncertainty (~3.0 ‰, 2σ). After the isotope data were collected, the section was imaged using an FEI Inspect-F SEM to check the placement and mineralogy of the NanoSIMS analysis spots.

Results: Oxygen isotope data (Fig. 3) were collected from 36 spots in two traverses across the layered rim, margin and interior of the CAI (Fig. 1). Six spots overlapped more than one mineral and are excluded from figure 3. The data are uniformly ^{16}O-rich with a limited range in $\Delta^{17}O$ of –20.2 ‰ to –27.6 ‰. Typical measurement uncertainties in $\Delta^{17}O$ are ~3.5 ‰ (2σ) (Fig. 3). In contrast to recently studied Allende CAIs A37, ALH and Egg-6 [7], we observe no statistically significant differences in $\Delta^{17}O$ between different CAI minerals or between the rim sequence, CAI margin and interior; melilite and spinel are equally ^{16}O-rich. The average $\Delta^{17}O$ from all analyses is -24.2 ± 0.6 ‰ (2SE).

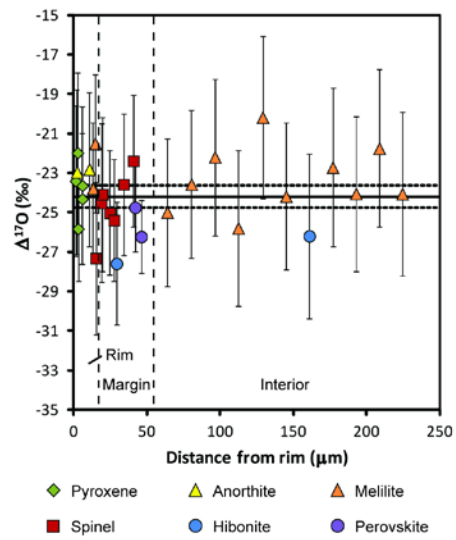

Figure 3. $\Delta^{17}O$ (‰) as a function of distance from the outermost rim of the CAI. The solid horizontal line is the average $\Delta^{17}O$ of all analyses, and the dashed horizontal lines show ±2 SE about the average.The vertical dashed lines denote the boundaries between the rim and margin (left) and the margin and interior of the CAI (right). Uncertainties are 2σ.

Conclusions: The oxygen and Mg isotope data from MUM-1 indicate this CAI experienced a relatively simple nebular history and provide no evidence for isotopic disturbance or sub-solidus re-equilibration. We did not observe the large mass-dependent fractionation effects (>15 ‰/amu) seen in some hibonite-rich Murchison CAIs [8]. The oxygen isotope characteristics of this Type A inclusion are most similar to CAIs from CR and CH chondrites [2-3], and contrast strongly with the complicated oxygen isotope zoning profiles observed in CAIs from CV and some CO chondrites [1, 9-10]. Together, the mineralogy and oxygen and Mg isotope data suggest that MUM-1 was isolated from the nebular gas at a relatively high nebular temperature and did not experience later reheating events commonly observed in other chondrite types.

References: [1] Simon, J. I. et al. (2011) *Science,* 331, 1175-1178. [2] Krot, A. N. et al. (2008) *The Astro. Journal,* 672, 713-721. [3] Makide, K. et al. (2009) *GCA,* 73, 5018-5050. [4] MacPherson, G. J. et al. (1983) *GCA,* 47, 823-839. [5] Grossman, L. (1980) *Ann. Review,* 8, 559-608. [6] Tanaka, T. et al., (1980) *LPS XI*, 1122-1124. [7] Simon, J. I. et al. (2013) *LPSC XXXIV*. [8] Ireland, T. R. et al. (1989) *Meteoritics,* 24, 279. [9] Aléon, J. et al. (2007) *EPSL,* 263, 114-127. [10] Itoh, S. et al. (2004) *GCA,* 68, 183-194.